Quest Journals
Journal of Research in Environmental and Earth Sciences
Volume 10 ~ Issue 12 (2024) pp: 35-53
ISSN(Online) :2348-2532
www.questjournals.org

Research Paper

Flood risk assessment using GIS and remote sensing in Tsholotsho District, Matabeleland North in Zimbabwe

Musekiwa Innocent. Maruza[1]*, Mkhokheli Sithole[2], Nkosinath Moyo[3]
[1]*Department of Geography and Geo-Information Sciences, Lupane State University, P.O Box 170, Lupane*
[2] *Institute of Development Sciences, National University of Science and Technology, P.O Box AC 939, Ascot, Bulawayo*
[3] *Department of Geospartial Science, National University of Science and Technology, P.O Box AC 939, Ascot, Bulawayo*

Abstract
Floods are one of the most widely distributed hazards globally, and their management is an essential issue of concern among all stakeholders, especially in developing countries. Flooding is one of the most significant natural hazards affecting the Tsholotsho District, causing widespread damage to infrastructure and the natural environment and endangering people's lives. This study assessed flood hazards and risk areas in the District using remote sensing (RS), Geographic Information Systems (GIS), and analytical hierarchy process (AHP). Six main factors were considered to identify flooding hazard wards in the District: drainage density (DD), flow length, elevation, Normalized difference, vegetation index (NDVI), slope, and distance from the river. The study also identified five flood risk zones: high, moderate, low, and very low. The result of the flood risk map revealed that the low-risk area was 433699.57 hectares (56%), the moderate-risk area was 278328.41 hectares (36%), and the very high risk was 41060.25 hectares (5%) of the District. The results indicate that low-lying areas, mainly adjacent to major rivers such as the Gwayi and Manzamnyama Rivers, are highly susceptible to flooding, exacerbated by land degradation and deforestation. The study highlights the critical role of integrating GIS and remote sensing in flood risk assessment, providing decision-makers with valuable insights for developing early warning systems, flood hazard zoning, and sustainable land management practices. Recommendations for improving flood resilience in Tsholotsho District include community-based disaster risk reduction programs and the implementation of adaptive infrastructure.

Keywords: *Geographic Information System, Flood risk assessment, Flood-prone areas, Flood hazard mapping, Remote sensing, Tsholotsho District*

***R**eceived 03 Dec., 2024; **R**evised 12 Dec., 2024; **A**ccepted 14 Dec., 2024 © The author(s) 2024.*
P**ublished with open access at **www.questjournas.org

I. Introduction

The frequency and intensity of disasters have been increasing worldwide, and many lives have been lost, property and infrastructure destroyed, and some economies have been adversely affected (Sibanda & Matsa, 2020). Natural disasters, especially flooding and drought, can directly and severely impact rural communities in Zimbabwe (Gwimbi, 2007). Flooding is one of the most destructive natural hazards globally, and its impacts are particularly severe in developing regions, where vulnerability to environmental disasters is exacerbated by poverty, inadequate infrastructure, and limited institutional capacity. In recent years, flooding has claimed thousands of lives, made hundreds of thousands of people homeless, and caused several hundred billion dollars in economic losses (Twumasi *et al.*, 2020). Flooding is becoming more severe and frequent due to climate change and increased human-induced land-use changes, which pressure river channels and cause changes in river morphology (Aramburú-Paucar *et al.*, 2024).

In the last 30 years, floods have been the most catastrophic natural disaster affecting, on an average, about 80 million people per year of the total population affected by any natural disaster, causing economic damage worth over US$11 billion annually around the world (Bhatt et al., 2014). Flooding is a natural part of the hydrological cycle but can potentially cause death, displacement, environmental damage, and economic losses (Anumveh et al., 2023). Flooding is one of the most common natural disasters, often with disastrous consequences,

affecting 170 million people worldwide yearly (Hagos *et al.,* 2022). Floods caused direct economic losses of USD 386 billion worldwide since 2001 (Siam et al., 2022). Flooding is becoming more severe and frequent because of climate change and increased human-induced land-use changes, which puts pressure on river channels and causes changes in river morphology (Hagos *et al.,* 2022). Floods have affected rural development in developing countries due to fatalities, injuries, and substantial economic losses on an annual basis (Gaston, 2009). Floods also seem to be a recurrent phenomenon in Southern Africa, and research has predicted their continued future occurrence (Dube, 2017). The Cyclone Eline-induced floods of 2000 affected the Sub-Saharan countries in the Zambezi Basin, claiming the lives of more than 700 people, causing homelessness to more than 500,000 people, and resulting in over US$1 billion in damage to infrastructure (Dube, 2017). Economic damage caused by floods negatively impacts human well-being, promoting long-term poverty in flood-affected regions (Siam et al., 2022).

Tsholotsho District, located in the semi-arid region of Matabeleland North, Zimbabwe, is prone to recurrent flooding, especially during periods of intense rainfall (Tshuma, 2021). Floods in this District cause significant damage to homes, farmland, and infrastructure, displacing communities and disrupting livelihoods. In recent years, climate change has intensified the frequency and severity of flooding events, heightening the need for effective flood risk management strategies (Ngulube, Tatano & Samaddar, 2024). The District is increasingly experiencing severe flood events that adversely impact the local communities, infrastructure, and environment. These floods result in loss of both human and animal life, displacement of residents, destruction of property, and disruption of livelihoods (Nji, Balgah & Vubo, 2019). Floods are among the most devastating natural disasters in Tsholotsho District, posing significant threats to lives, property, and livelihoods. The District has been experiencing severe flooding disasters, resulting in damaged property, people's livelihoods, and, in extreme events, loss of life (Tshuma, 2021). The geographical location, topography, and observed land use/ land cover changes (LULC) contribute to the District's vulnerability to flooding (GOZ, 2017). These attributes necessitate a detailed assessment to identify and mitigate flood risks effectively. More comprehensive and accurate flood hazard data in the Tsholotsho District must be provided (Zimbabwe Human Rights Commission, 2015). Understanding the spatial extent and drivers of flood risk is crucial for formulating effective adaptation strategies to reduce the District's exposure to flood hazards.

Tsholotsho District faces unique flood risks due to its topography, proximity to major rivers such as the Gwayi and Manzamnyama, and socioeconomic characteristics (Tshuma, 2021). Flooding in Tsholotsho mainly occurs along the Gwayi and Zombani Rivers, near Gariya Dam, and other low-lying areas. These rivers seasonally burst, leaving a trail of severe disasters, impacting human settlements, infrastructure, and livelihoods (Dube et al., 2018). Low-lying areas and poorly drained soils make certain parts of the District particularly susceptible to inundation, while deforestation, land degradation, and unsustainable agricultural practices exacerbate the effects of floods (Dube et al., 2018).

Despite frequent flooding events, more research is needed on the District's spatial and temporal patterns of flood risk. Existing flood management strategies are primarily reactive, focusing on post-disaster response rather than risk reduction (Tirivangasi, Nyahunda & Mabila, 2021). A lack of detailed flood risk assessments and inadequate early warning systems further undermine the District's ability to prepare for and mitigate flood events. Traditional methods of flood management, largely reactive, need to be revised to address the growing flood risks in the District. Current flood management practices are often reactive rather than proactive, and local authorities need more tools and data to implement effective flood risk reduction strategies. Therefore, a more comprehensive, proactive, and data-driven approach to flood risk assessment is essential. Assessing flood risk is challenging due to complex interactions among flood susceptibility, hazard, exposure, and vulnerability parameters (Siam *et al.,* 2022). Despite the recurring nature and devastating consequences of floods, there needs to be more comprehensive flood hazard assessments and accurate mapping of flood-prone areas in Tsholotsho District. This gap in knowledge and resources hampers efforts to build flood resilience and protect vulnerable communities. Using Geographic Information Systems (GIS) and remote sensing technologies offers a powerful approach to assess and map flood hazards accurately (Mojaddadi et al., 2017). These technologies can provide detailed spatial and temporal data on flood patterns, identify high-risk areas, and support the development of predictive models for flood risk assessment (Singh & Kumar, 2017). However, these advanced tools have limited application in the context of Tsholotsho District. Advancements in Geographic Information Systems (GIS) and remote sensing offer powerful tools for assessing flood risk, particularly in areas with limited ground-based data (Manyangadze et al., 2022). These technologies allow for integrating and analyzing spatial data, such as rainfall patterns, topography, and land use/cover, to model flood hazards and identify vulnerable areas (Samu & Kentel, 2018). Remote sensing provides multi-temporal satellite imagery, enabling monitoring of land use changes and water dynamics over time, while GIS facilitates the spatial analysis necessary to create detailed flood risk maps (Wudineh, 2023).

This research paper thus addresses the critical need for a systematic and scientific approach to flood hazard assessment and mapping in the Tsholotsho District. It utilizes satellite imagery and remote sensing data to enhance understanding of flood patterns and risks and develop detailed flood hazard maps using GIS and remote sensing techniques. The maps will delineate flood zones and categorize them based on the hazard level.

By leveraging GIS and remote sensing technologies, the study seeks to fill the existing knowledge gaps, provide actionable insights for flood risk management, and contribute to developing sustainable and resilient communities in the District. GIS and remote sensing provide cost-effective and efficient methods for conducting flood risk assessments, especially in regions where traditional ground-based data collection is challenging. This study will generate accurate, up-to-date flood risk maps and contribute to a more proactive flood management approach in Tsholotsho. The insights gained from this research have broader applications for flood-prone areas across Zimbabwe and Southern Africa, where similar environmental and socioeconomic conditions prevail.

Globally, GIS and remote sensing have been used to identify flood extents and impacts, to inform flood and evacuation models, and as part of emergency response activities (Kourgialas & Karatzas, 2011). GIS and remote sensing technologies offer advanced capabilities for detailed spatial analysis and visualization of flood hazards in the District. These technologies can provide high-resolution data, enabling precise identification of flood-prone areas and enhancing the accuracy of flood risk assessments. By conducting a thorough flood hazard assessment and creating detailed flood hazard maps, this study will support proactive flood management strategies in Tsholotsho District. The Civil Protection Unit (CPU), local authorities, and NGOs in disaster risk reduction can use the information to implement early warning systems, prepare contingency plans, and design effective flood mitigation measures. Understanding the current flood hazards and predicting future scenarios is crucial for developing adaptive strategies to cope with the impacts of climate change on flood risks in Tsholotsho District.

This study seeks to leverage the capabilities of GIS and remote sensing to assess flood risks in Tsholotsho District and improve flood management and mitigation efforts. The study utilizes Geographic Information Systems (GIS) and remote sensing technologies to assess flood risk in Tsholotsho District, aiming to enhance flood management and mitigation strategies. By integrating hydrological data, satellite imagery, and spatial analysis techniques, this research will identify flood-prone zones, assess the factors contributing to increased flood vulnerability, and develop flood risk maps to inform decision-making processes. In doing so, this thesis will contribute to a more nuanced understanding of flood dynamics in semi-arid regions and provide practical recommendations for enhancing flood resilience in Tsholotsho District.

The study contributes to the attainment of the overall outcome of the Sendai Framework for Disaster Reduction. The Sendai Framework for Disaster Reduction aims to substantially reduce disaster risk and losses in lives, livelihoods, health, and the economic, physical, social, cultural, and environmental assets of persons and communities (Ma et al., 2024). The primary beneficiaries of this research will be the local communities in Tsholotsho District. By identifying high-risk areas and recommending appropriate mitigation measures, the study will minimize the chance of community resilience, reduce loss of life, and minimize property damage. The flood mapping exercise aims to identify flood-safe areas (evacuation centers) in the case of flood disasters. The findings of this dissertation will provide valuable insights for policymakers, planners, and development agencies. The detailed flood hazard maps and risk assessments will be critical tools for informed decision-making and sustainable land use planning. This research will contribute to the broader knowledge of flood hazard assessment and management, mainly using GIS and remote sensing technologies in developing regions.

II. Materials and Methods

2.1 Study area

The study was conducted in the Tsholotsho district, one of the seven districts in Matabeleland North province in Zimbabwe. The District falls under Agro-ecological Region Five, generally flat and dominated by poorly drained Kalahari sand soils (Tshuma, 2021). It is about 114km west of Bulawayo and borders Lupane to the north, Umguza to the east, Hwange to the northwest, and Bulilimangwe to the south. Part of the Tsholotsho district drains into the Gwayi River, and the other part drains into the Manzamnyama River (Dube, 2017). Gwayi River is part of an international basin, the Zambezi, and it forms one of the seven catchments in Zimbabwe. Land use in the study area includes settlement, croplands, grazing, and woodland. Agriculture is the primary source of livelihood in Tsholotsho. Tsholotsho district has a population of 119 681 (Zimstat, 2022), with a population density of 16 persons/km^2 (Dube, 2017). Tsholotsho is home to three ethnic groups: Ndebele (96%), Kalanga (3%), and San (1%) (Tshuma, 2021). Tsholotsho district is prone to flash floods, which can be attributed to poor drainage and the fact that the land is relatively flat (Nyoni et al., 2019). Wards such as Sipepa, Jimila, and Mbiriya are highly prone to these flash floods (Tshuma, 2021). In the Sipepa and Jimila wards, the areas along the Gwayi River are mostly affected by floods. Cultivating along fertile floodplains will also contribute to the situation (Tshuma, 2021). The at-risk population is situated in a low-lying area that is very low in height above the river channel base (Dube, Wedawatta & Ginige, 2021). The District has been experiencing floods almost every year, though with varying magnitudes (Dube, 2017), in low-lying areas and flood plains along the rivers. In 2017, according to a report by Civil Protection Zimbabwe, one of the areas worst affected by cyclone Dineo was Tsholotsho District, where the Gwayi River and its tributaries burst their banks, inundating homes, fields, schools and infrastructure, and sweeping away livestock (Floodlist, 2017). The same areas were affected by floods in 2001 and 2013, leading to communities being evacuated and settled at Sipepa Rural Health Centre (ibid). Since

flooding is the outcome of highly complex and intricate dynamic processes, it is nearly impossible to prevent it from occurring; hence, flood risk reduction has become one of the significant challenges worldwide (Siam et al., 2022). The emergence of various remote sensing and geospatial techniques has enabled researchers and practitioners to assess flood risk more accurately (Rahman et al., 2021). A comprehensive flood risk assessment plays a vital role in the overall flood risk management system, which requires quantifying flood hazard, exposure, and vulnerability (Siam et al., 2022). The study utilizes advanced GIS and remote sensing technologies to collect, process, and analyze spatial data related to flood hazards in the District, hence creating detailed and accurate flood hazard maps that delineate flood-prone areas and categorize them based on different levels of risk. There is a need to develop flood risk maps and vulnerability assessments that can inform early warning systems and disaster preparedness in Tsholotsho District.

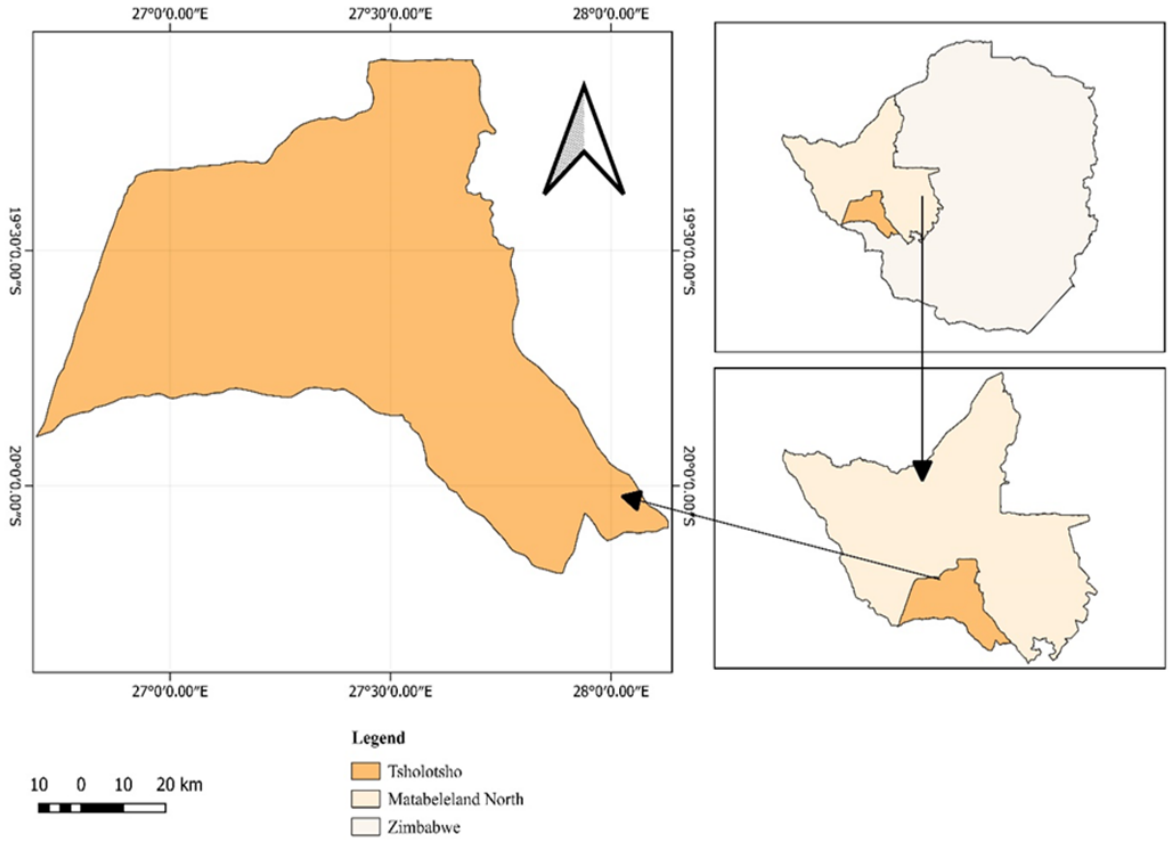

Figure 1: Map of Tsholotsho District

2.2 Research Approach

Significant factors were identified through a literature review, relevant layers were identified through a literature review, and relevant layers were determined. Geoprocessing operations were applied to each input layer, reclassified, and standardized to enable comparability. A standard scale of 1 to 5 was adopted, with higher values indicating high-risk flood locations. Factor weights were derived using AHP, based on a pairwise comparison matrix informed by literature (Akbulut *et al*., 2018). The weighted overlay method was then employed to combine the input maps, ultimately producing a final flood hazard map highlighting both less flood-prone and flood-prone areas. A detailed explanation of the methodology is provided in the following sections.

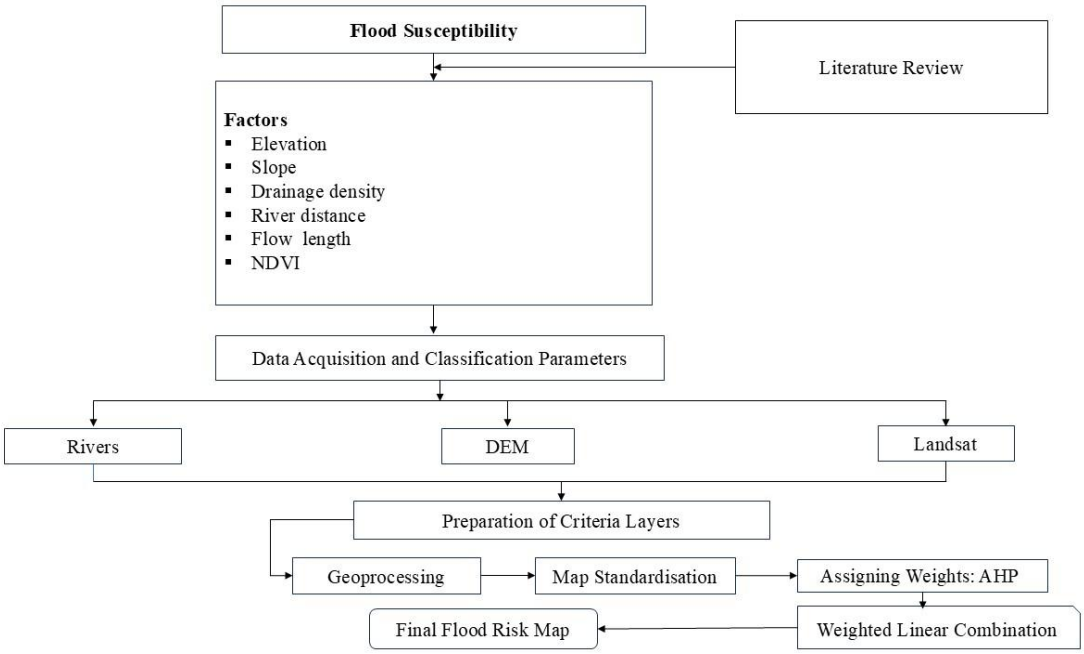

Figure 2. Overall flowchart of the research methodology

2.3 Determining Flood Susceptibility Criteria and Factors

GIS-based flood susceptibility analysis requires a thorough analysis of multiple factors to determine an area's susceptibility (Karna et al., 2023). Multi-criteria evaluation (MCE) integrates conflicting and complementary criteria for more informed decision-making (Akbulut et al., 2018). This method synthesizes complex factors into a composite map to identify vulnerable sites (Wu & Liang, 2012). This study evaluates six environmental factors to identify flood-vulnerable areas within the Tsholotsho district.

2.3.1. Elevation

Elevation is essential in controlling the direction and depth of water levels during overflow (Diriba et al., 2024). Lowland locations are more vulnerable to flooding as water moves from higher to lower elevations (Chakraborty & Mukhopadhyay, 2019). The elevation map is made possible by reclassifying the DEM (Osman & Das, 2023). A Digital Elevation Model (DEM) specifies the elevation of any point in a particular area at a specific spatial resolution as a digital file, which is used to characterize topography. A DEM is required for raster-based hydrological analysis in a GIS.

2.3.2. Slope

Gradient plays a crucial role in determining the water flow speed and duration. Water moves more slowly and stays longer on flatter surfaces, making these areas much more prone to flooding than steeper surfaces (Diriba et al., 2024). The slope is another crucial flood-triggering parameter (Mitra & Das, 2023). The slope directly impacts drainage and runoff accessibility (Kaya & Derin, 2023). Slope also affects the volume and velocity of surface runoff and groundwater infiltration (Osman & Das, 2023).

2.3.3 Drainage density

Drainage density is one of the key variables that lead to floods. The runoff rate is critical for high drainage density (Akallouch *et al*., 2024). Areas with high drainage density tend to have more channels to transport water quickly. This rapid runoff can reduce infiltration and lead to quicker water accumulation downstream, heightening flood risk, particularly during heavy rainfalls (Li *et al*., 2016). Osman and Das (2023) used drainage capability to integrate the combined effect of elevation and drainage density for food hazard mapping. Many approaches have been used to determine drainage density, with a computer tool (GIS software) playing a significant role (Diriba *et al*., 2024).

2.3. 4 Distance to river

The distance from the river network component is crucial in determining the food risk zones and the food hazard index (Ayenew & Kebede, 2023). Flood hazards are most severe in locations near river networks, according to Osman and Das (2023). In contrast, the effect of this parameter reduces as one advances away from the riverbed.

2.3.5 Flow Length of a river

Longer flow lengths typically mean water travels a greater distance, which can affect its velocity depending on the river gradient. In flatter regions with long flow lengths, water moves more slowly, potentially allowing for more accumulation in upstream areas and increasing the risk of prolonged or recurrent flooding (Wondim, 2016). In contrast, shorter rivers with steep slopes tend to have faster water flow, often leading to flash floods downstream after intense rainfall (Molnar-Tanaka & Surminski, 2024).

2.3.6 Normalized Difference Vegetation Index (NDVI)

The NDVI index assesses vegetation's greenness and surface water's presence. Variations in NDVI values over time reveal changes in vegetation and surface water, which can help understand the relationship between flooding and vegetation in a region (Shahabi et al., 2022; Tehrany et al., 2013). Increased vegetation cover reduces the likelihood of flooding.

2.3.7 Geospatial data

This study was primarily supported by geospatial datasets collected from various sources (Table 1). These datasets included the 30m-resolution SRTM Global Digital Elevation Model, Landsat 9 (30m resolution) (DEM), and river data. All data were projected to the WGS 1984 spheroid, Universal Transverse Mercator (UTM) Zone 36 South, using ArcMap 10.2.

Table 1. Data used in spatial analysis

Data type	Source type	Format
DEM (SRTM)	USGS (30 m) https://earthexplorer.usgs.gov/	Raster
Landsat 9	USGS (30 m) https://earthexplorer.usgs.gov/	Raster
Rivers	DIVA-GIS (www.divangis.org/datadown)	Vector
Wetlands	Environmental Management Agency	

2.3.8 Geoprocessing

An elevation map was generated from the DEM and categorized into five classes: very high (948–1004 m), high (1004–1046 m), medium (1046–1105 m), low (1105–1180 m), and shallow (1180–1308 m) (see Table 2).

The DEM was converted into a slope map using the Spatial Analyst tool in ArcMap 10.5. Risk levels classified the slope: <5% as very high risk, 6.80–13.46% as high risk, 13.46–28.86% as moderate risk, 28.86–30.55% as high risk, and >30% as very high risk (Table 2).

Buffer zones were delineated around rivers, with five suitability categories: very high risk (0–903 m), less suitable (903–1829 m), moderate risk (1829–2710 m), low risk (2710–3843 m), and shallow risk (3843–7141 m) (Kumar & Deswal, 2022; see Table 2).

The flow length was calculated using ArcMap drainage tools, with classes defined as very high (0–20,137.02 m), high (20,137.02–43,935.32 m), medium (43,935.32–70,174.47 m), low (70,174.47–100,685.11 m), and shallow (0–20,137.02 m) (Table 2).

Lastly, a drainage density map was produced, with classes designated as very low (0–0.26 km/km²), low (0.26–0.41 km/km²), medium (0.41–0.53 km/km²), high (0.53–0.67 km/km²), and very high (0.67–1.00 km/km²) (Table 2). Areas with the highest drainage density were identified as more susceptible to flooding.

An NDVI layer was created with classes defined as very high (-0.14 - 0.11), high (0.11 - 0.13), medium (0.13 - 0.14), low (0.14 - 0.16), and very low (0.16 - 0.35) (Table 2)

2.4 Standardisation

Each layer was reclassified based on the criteria outlined in Table 2 to ensure consistency across all datasets. This reclassification process standardized each raster map into five distinct suitability classes: (1) shallow risk, (2) low risk, (3) moderate risk, (4) high risk, and (5) very high risk. By creating uniform classes across layers, the reclassification facilitated a direct comparison of different factors, enabling more precise identification of risk areas.

Table 2. Description and classification of analysis criteria of selected factors to identify flood-susceptible areas.

Data layer	Unit	Range	Susceptibility	class
Elevation	m	335-843	Very High	5
		843-1127	High	4
		1127-1367	Moderate	3
		1327-1626	low	2
		1626-2381	Very low	1
Slope	degree	0-6.80	Very High	5
		6.80-13.46	high	4
		13.46-28.86	Moderate	3
		28.86-30.55	low	2
		30.55-7.83	Very low	1
Flow length	m	0 - 20137	Very High	5
		20,137 - 43935	High	4
		43,935 - 70174.	Moderate	3
		70174- 100685	Low	2
		100685 - 155604	Very Low	1
Distance to river	m	0-903	Very High	5
		903-1829	High	4
		1929-2710	Moderate	3
		2710-3843	low	2
		3843-7141	Very low	1
NDVI	level	-0.14 - 0.11	Very High	5
		0.11 - 0.13	High	4
		0.13 - 0.14	Moderate	3
		0.14 - 0.16	low	2
		0.16 - 0.35	Very low	1
Drainage Density	Km2	0–0.26	Very High	5
		0.26–0.41	High	4
		0.41–0.53	Moderate	3
		0.53–0.67	Low	2
		0.67–1.00	Very Low	1

2.5 Analytical Hierarchy Process

Recognizing that not all factors hold equal significance (Adimi et al., 2018), the analytic hierarchy process (AHP), established by Saaty (2008), was applied to assign weights. This method involves pairwise comparisons of criteria based on their relative importance to the main objective, using a 9-point scale developed by Saaty (1997). This scale, ranging from 1 (equal importance) to 9 (extreme importance), is illustrated in Table 3. The AHP approach allows decision-makers to independently assess each criterion's contribution to the objective, simplifying the decision-making process.

Table 3. The scale of pairwise comparison scale for AHP preferences

Number	Priority
1	Equally preferred
3	Moderately preferred
5	Strongly preferred
7	Very strongly preferred
9	Extremely preferred
2,4,6,8	The importance is between two degrees

An Excel-based pairwise comparison matrix by Goepel (2013), downloaded from https://bpmsg.com/, was used to calculate weights. These weights were determined based on literature and environmental regulations. The consistency of each factor's importance was verified using the consistency ratio, with the consistency index (CI) calculated as follows:

$$CI = \frac{\lambda max - n}{n - 1}$$

In this context, λmax represents the highest eigenvalue of each factor within the matrix, and n denotes the matrix size.

The consistency ratio (CR) was then calculated as the ratio of the consistency index (CI) to the random consistency index (RI) to evaluate the reliability of the matrix judgments. For the matrix to be considered consistent, the CR needed to be less than 0.1 (Saaty, 1997). The following formula gives the consistency ratio (CR):

$$CR = \frac{C1}{RI}$$

2.5.1 Weighted Linear Combination (WLC)

The calculated weights were then applied to determine the overall flood susceptibility using the weighted linear combination method in ArcMap's Spatial Analyst tool, resulting in the final suitability map. This approach follows a general modeling technique based on the susceptibility map equation outlined by Siefi et al. (2017). The total susceptibility was calculated as follows:

$$S = \sum (Wi * Xi)$$

In this formula, S represents the total suitability score for residential installation; Wi denotes the weight of each selected suitability criteria layer, and Xi is the assigned score for each sub-criterion within susceptibility y criteria layer i.

2.6 Data analysis

Following the creation of the flood susceptibility map, spatial analysis was conducted to determine the area covered by each susceptibility class. Using GIS tools, the total area in square kilometers was calculated for each class (highly suitable, shallow risk, low risk, moderate risk, high risk, and very high risk). These values were then converted into percentages to illustrate the proportion of land designated for each susceptibility level. Bar charts and pie charts were generated to visualize the distribution of suitable and unsuitable areas, providing a clear, comparative view of each class's contribution to the overall study area. This graphical representation aids in quickly identifying flood-suspecting zones and informs decision-making by urban local authorities.

2.7 Flood hazard mapping

This research developed a flood hazard map for the Tsholotsho district by integrating the six flood-affected strata, similar to other food hazard research. According to many experts, flood-prone areas have a mix of shallow elevation, low slope, and high drainage density (Natkaniec & Godyń, 2024). Using the natural breaking slope approach in the "ArcGIS 10.4.1 environment," the hazard was divided into five main groups: high, high, moderate, low, and shallow hazard zones. Weighting strategies rank the relative value of each factor to another. In weighted overlay, the higher the weight, the more essential the component is compared to the other factors (Wondim, 2016). The final food hazard map was created by overlapping the six floods and their associated coefficients for the Tsholotsho district.

III. Results and Discussion

Flood risk assessment must recognize the increasing interconnectivity between physical infrastructure and economic systems and the critical role of human factors in determining flood risk (Ajjur & Al-Ghamdi, 2022). The flood risk assessment in Tsholotsho District, conducted using GIS and remote sensing, revealed significant findings regarding flood-prone areas, the factors influencing flood risks, and the vulnerability of local communities and infrastructure. GIS mapping and analysis identified specific flood-prone zones within the Tsholotsho District, primarily concentrated along the Gwayi and Manzamnyama river systems. These areas were characterized by low elevations, flat terrain, and proximity to major water bodies, making them particularly susceptible to flooding during the rainy season, according to the AHP weights and rating, drainage density, distance to the river, elevation, and flow length significantly impact flood incidence in the District. Although the District has 22 wards, the research revealed that Wards 5, 6, 7, and 8 were the most flood-prone. The research identified Ward 7 had parts flood-prone areas, Ward 5 (Sipepa) and Ward 6 (Jimila) that were very highly flood-prone areas, Ward 5 (Sipepa) and Ward 6 (Jimila) had parts of these wards ranging from medium to high risk of flooding. The flood risk maps indicate that roughly 25% of the District's land area falls within high—and moderate-risk zones, with a high risk of annual or seasonal flooding.

3.1 Parameters used in the analysis of flood susceptibility

3.1.2 Elevation

The elevation map of the study area is categorized into five distinct classes, with the areas from 335 to 843 meters above sea level being very high flood-prone areas. These areas were mainly the floodplains of the main rivers in the District. The areas 843 to 1127 meters above sea level were high flood-prone areas. Most parts of wards 5, 6, 7, and 8 had most parts falling under the high flood-prone areas. The areas 1127-1367 meters above

sea level were moderate flood-prone areas. These areas are usually under flood after excessive rainfall, but the damage is mild compared to the high and high categories. Elevations, in general, are a critical factor in determining which areas are at risk of flooding (Bora et al., 2023). Elevation is used to model flood risk because it affects water flow during flood events (Al-Kindi & Alabri, 2024). Areas with higher elevations are less prone to flooding than areas with lower elevations. Usually, water flow is from high-altitude areas towards low-altitude areas so that low-lying areas may get flooded rapidly (Liuzzo et al., 2019). In the context of global climate change, the frequency and duration of precipitation have increased, leading to higher flood risks in watersheds and low-lying areas (Gu & Liu, 2024). The connection between flood risk and land elevation is critical in flood risk assessment, as areas with lower elevations are naturally more susceptible to flooding (Government of India, 2008). Flooding is proportional to elevation in an inverse manner (Bora et al., 2023). Mojaaddadi et al. (2017) emphasize that elevation is a crucial factor influencing flood events, as water flows from higher to lower elevations. Low-lying areas are especially susceptible to flash flooding compared to higher altitudes (Subraelu et al., 2023). Lower-lying areas, such as floodplains, river basins, and coastal zones, are more susceptible to flooding as they are prone to water accumulation from rainfall, river overflow, and storm surges (Al-Kindi & Alabri, 2024). In areas with steep slopes, rainwater quickly flows downhill, potentially reducing the chance of local flooding but increasing downstream flood risk. In addition, areas at lower elevations are more likely to experience severe flooding, particularly in areas where water cannot quickly drain away (Al-Kindi & Alabri, 2024). The higher the elevation, the less likely flooding will occur; conversely, the lower the elevation, the greater the likelihood of flooding (Bora et al., 2023). (Fig. 3).

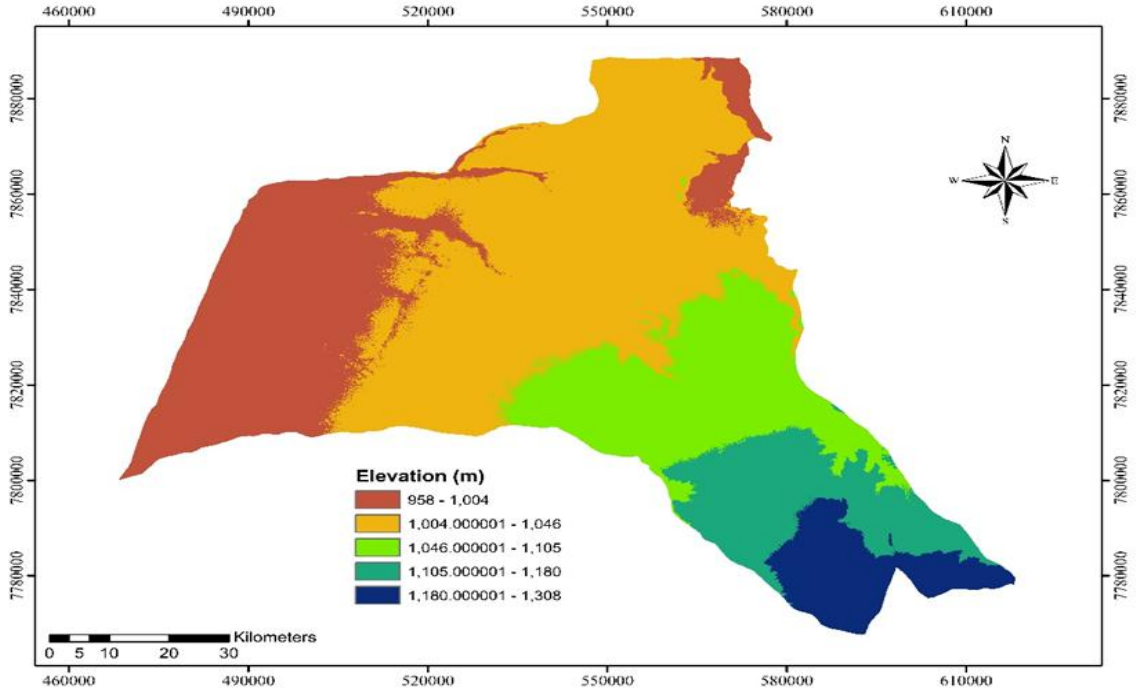

Figure 3. Elevation Map of Tsholotsho

As a result, in Tsholotsho district, areas with low elevations are highly vulnerable to flooding, as indicated on the above map. The probability of flooding is higher in low-elevated areas than in high-elevation areas (Rahman et al., 2023).

3.2.1 Slope

Slope values are measured in degrees, and the slope map for the study area, generated using ArcGIS 10.2 with ASTER DEM data, is classified into five categories: very high (0–1.78°), high (1.78–3.39°), medium (3.39–5.33°), low (5.33–9.52°), and very low (9.52–41.16°) (Fig. 4). Areas with lower slopes are disproportionately affected by flooding. Low topographic steepness and flatness reduce runoff and infiltrate the area after occasionally producing a state where water is stored. In flood risk assessment, the slope is significant because the speed of flowing water and the amount of water that can get into the ground is controlled by the area's slope (Bora et al., 2023). The slope is one of the most critical factors in hydrological studies because it controls surface runoff and water flow intensity that incites soil erosion and vertical infiltration process (Rahman et al., 2023). According to Das et al. (2021), the risk of flooding increases as the slope decreases. The area with a higher slope gradient has low exposure to flooding, while the area with a low slope gradient is highly exposed to flooding (Liuzzo et al., 2019). Flat surfaces can cause runoff to flow rapidly, heightening flood vulnerability, whereas rough surfaces slow down runoff, delaying flooding (Rahman et al., 2023).

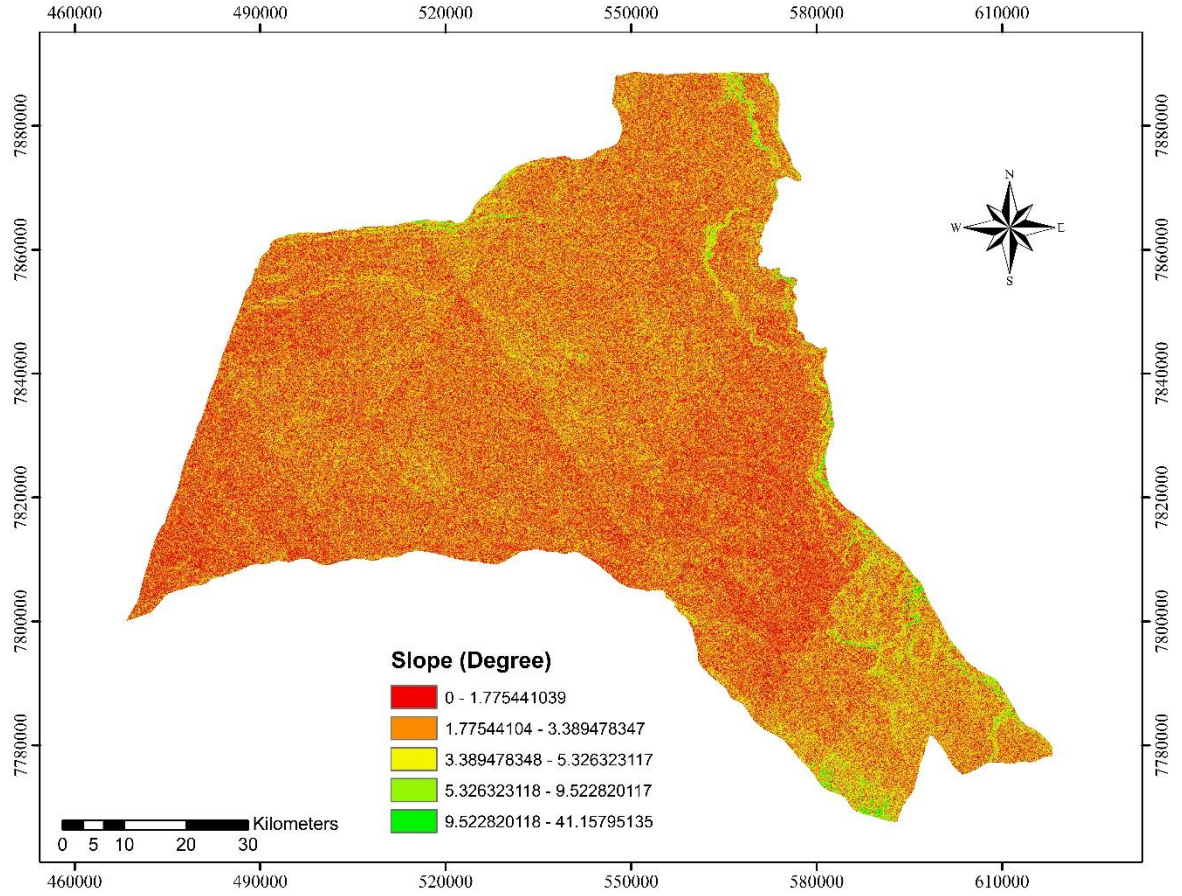

Figure 4. Slope Map of Tsholotsho

As a result, in Tsholotsho district, areas with the lowest slope are disproportionately affected by flooding.

3.2.2 Drainage Density

Drainage density is a significant factor in the occurrence of floods. The drainage network data was converted into a compatible GIS format and created in ArcGIS layers. The drainage density map of the study area is divided into five categories: very low (0–0.26 km/km²), low (0.26–0.41 km/km²), medium (0.41–0.53 km/km²), high (0.53–0.67 km/km²), and very high (0.67–1.00 km/km²) (Fig. 5). Areas with the highest drainage density are particularly vulnerable to flooding. Drainage density is characterized as the entire length of the waterways and streams in a river basin divided by the whole area of the basin (Rahman et al., 2023). When drainage density is high, runoff occurs significantly, and the likelihood of flooding increases (Bora et al., 2023). Drainage density is an important metric since it shows a catchment's potential for runoff (Vijith & Satheesh, 2006). A greater drainage density suggested a greater possibility for runoff. Drainage density is another significant factor in flood occurrences, as higher drainage density leads to faster runoff and a higher likelihood of flooding (Saha, Gayen & Bayen, 2022).

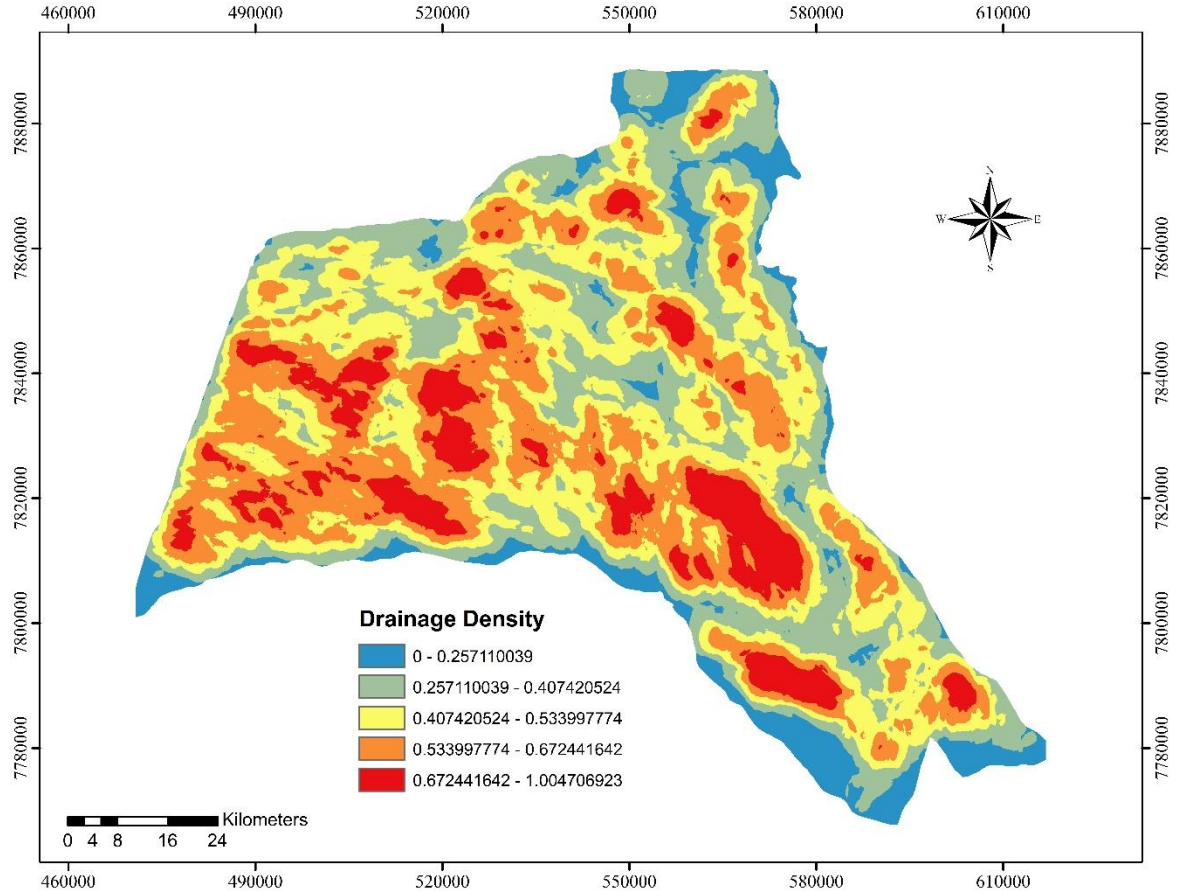

Figure 5.Drainage Density Map of Tsholotsho

In the District, the areas with the highest drainage density are disproportionately affected by flooding, as indicated on the map. Areas of higher drainage density have greater chances of flooding, whereas areas of lower drainage density have fewer chances of flooding (Rahman et al., 2023).

3.2.3 Distance from River

The thematic layer for distance from rivers is classified into five categories: very high (0–386.88 m), high (386.88–870.47 m), medium (870.47–1426.61 m), low (1426.61–2466.34 m), and shallow (2466.34–6165.86 m) (Fig.6 and Table 4). Consequently, areas close to rivers are more susceptible to floods. The distance from the rivers is critical in determining the flood risk zone (Bora et al., 2023). The distance from rivers is crucial in determining flood risk zones, as areas near river networks are at a higher risk of flooding. The further away from a river, the lower the flood risk (Chapi et al., 2017). Flood hazard has a more significant impact in areas adjacent to the river network, while its effect diminishes gradually as one moves away from the river (Bora et al., 2023).

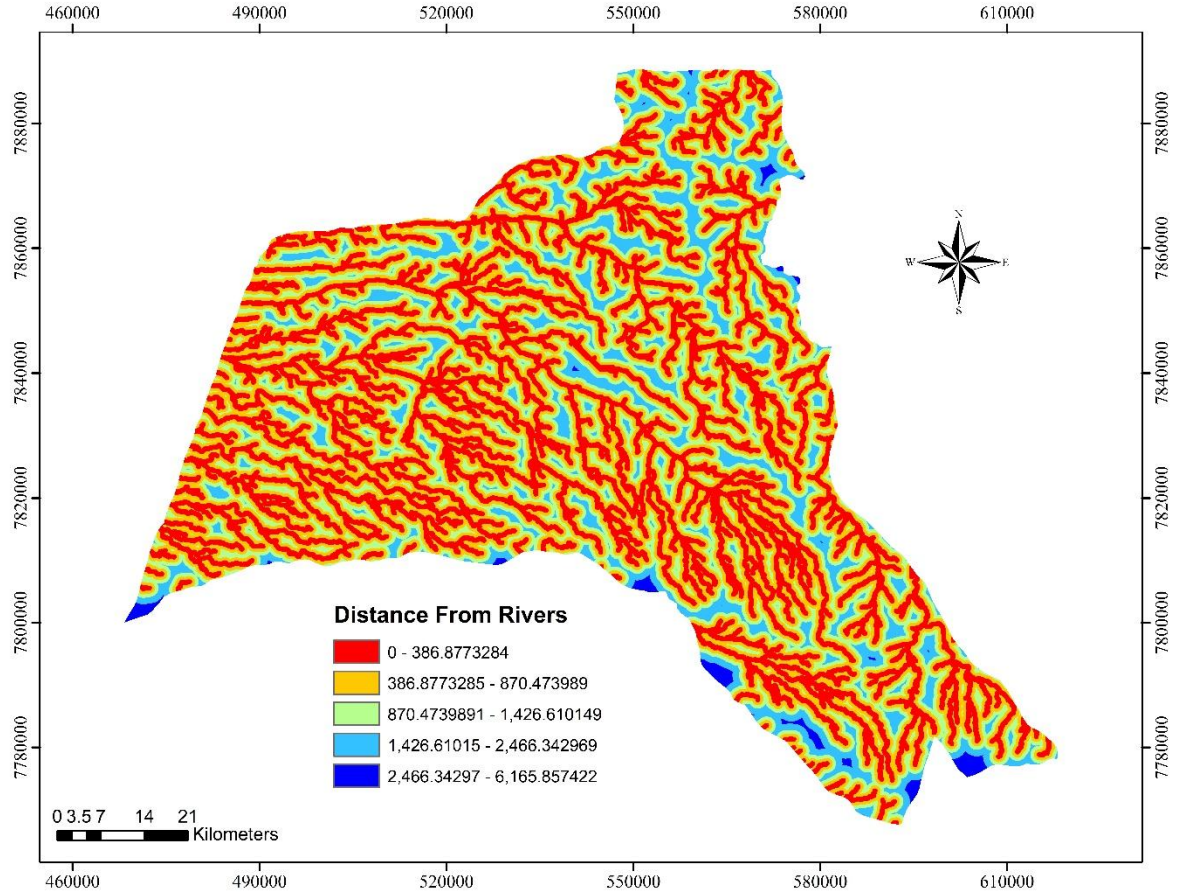

Figure 6. Distance from Rivers Map of Tsholotsho

As a result, areas near the main rivers are more vulnerable to flooding than rivers places further away from them.

3.2.4 Flow Length

Flow length represents the distance water travels from each cell to the flow outlet. Flow length is a factor used to determine the risk of flooding and erosion, with longer flow lengths indicating a higher risk. Areas with shorter flow lengths have higher flood risk, while longer flow lengths reduce flood vulnerability (El-Fakharany & Mansour, 2021). The flow length map is categorized into five classes: very high (0–20,137.02 m), high (20,137.02–43,935.32 m), medium (43,935.32–70,174.47 m), low (70,174.47–100,685.11 m), and shallow (0–20,137.02 m) (Fig. 7 and Table 4). The figures above show that the areas with a flow length of 0–20,137 meters were very high flood-prone areas. The areas with 20,137–43,935 meters flow length were high flood-prone areas, and 43,935–70,174 meters flow length were medium flood-prone areas.

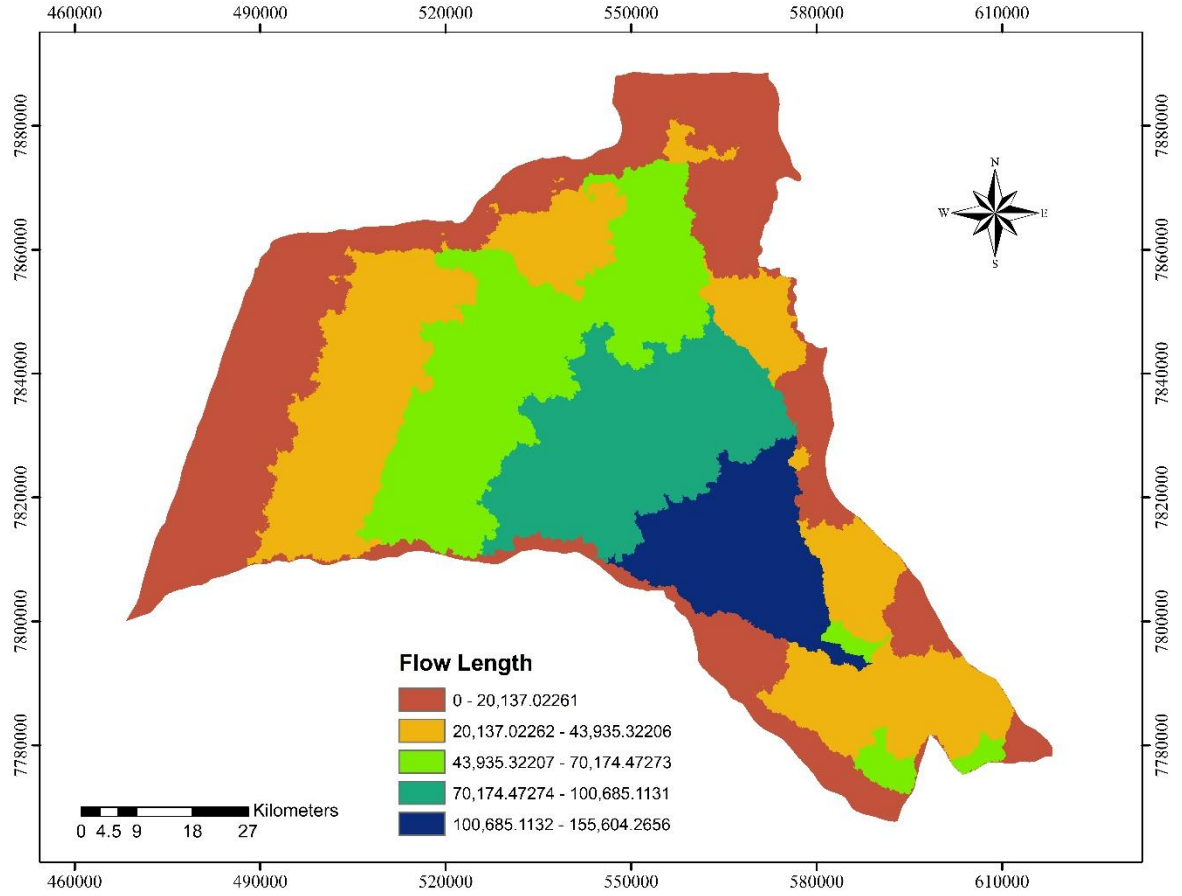

Figure 7. Flow length Map of Tsholotsho

3.2.5 Normalized Difference Vegetation Index (NDVI)

The NDVI thematic map was generated using Landsat 8 satellite data in ArcGIS 10.4 (Fig. 8 and Table 4). Remote sensing analysis of land cover types revealed that areas with minimal vegetation, particularly deforested or agricultural lands, exhibited higher flood susceptibility. The degradation of natural vegetation has reduced the land's capacity to absorb rainwater, contributing to increased runoff. In contrast, areas with dense forest cover displayed lower flood risk, emphasizing the role of vegetation in mitigating flood hazards. Normalized difference vegetation index (NDVI) is another main ecological flood-causing factor (Rahman et al., 2023). The nexus between flooding and the NDVI explores how flooding impacts vegetation health and how NDVI, a remote sensing index, can monitor flood-affected areas (Rahman et al., 2023). The NDVI is a statistical indicator used to determine the amount of green on the land surface and the presence or absence of bodies of water (Bora et al., 2023). Variations in NDVI values over time reveal changes in vegetation and surface water, which can help understand the relationship between flooding and vegetation in a region (Shahabi et al., 2021; Tehrany et al., 2013). The average value of the NDVI is ranging from −1 to +1 (Ziwei et al., 2023). An increment in the density of vegetation cover is believed to decrease the likelihood of flooding in the region (Bora et al., 2023).

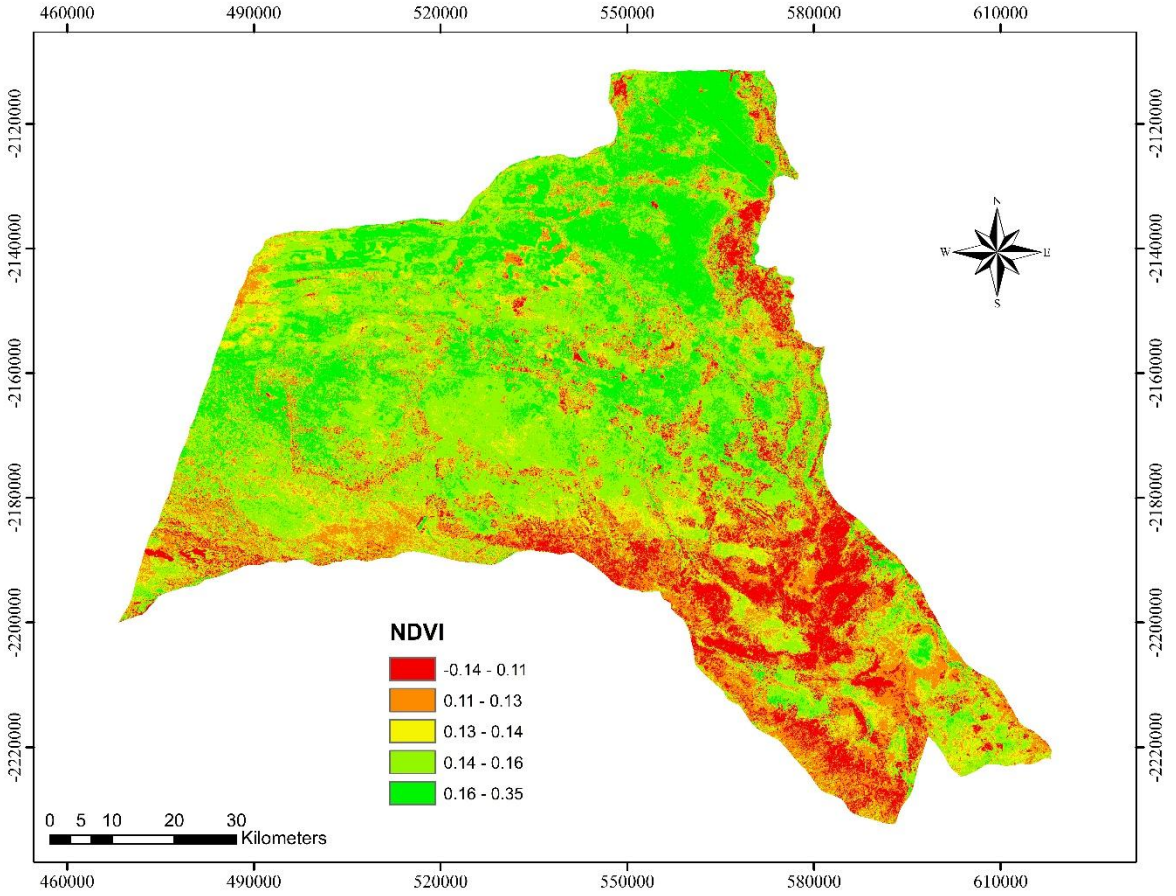

Figure 8. NDVI Map of Tsholotsho

The NDVI-flood nexus highlights how remote sensing can be used to monitor flood impacts on vegetation, supporting flood response, recovery, and ecosystem management efforts.

The factors contributing to flooding in Tsholotsho District, such as elevation, slope, flow length, distance to river, NDVI, and drainage density, were selected. Multi-criteria analysis (MCA) was applied to create the Tsholotsho district flood maps in GIS. MCA integrates the spatial data to describe the causative factors of flooding in the District.

Table 4. Selected parameters for flood susceptibility with their AHP weights and rating of sub-classes of each parameter.

Data layer	**Unit**	**Class**	**Suitability Susceptibility**	**Rating**	**Weight (%)**
Elevation	m	335-843	Very High	5	20
		843-1127	High	4	
		1127-1367	Moderate	3	
		1327-1626	low	2	
		1626-2381	Very low	1	
Slope	degree	0-6.80	Very High	5	10
		6.80-13.46	high	4	
		13.46-28.86	Moderate	3	
		28.86-30.55	low	2	
		30.55-7.83	Very low	1	
Flow length	m	0 - 20137	Very High	5	20
		20,137 - 43935	High	4	
		43,935 - 70174.	Moderate	3	
		70174- 100685	Low	2	

		100685 - 155604	Very Low	1	
Distance to river	m	0-903	Very High	5	20
		903-1829	High	4	
		1929-2710	Moderate	3	
		2710-3843	low	2	
		3843-7141	Very low	1	
NDVI	level	-0.14 - 0.11	Very High	5	15
		0.11 - 0.13	High	4	
		0.13 - 0.14	Moderate	3	
		0.14 - 0.16	low	2	
		0.16 - 0.35	Very low	1	
Drainage Density	Km2	0–0.26	Very High	5	20
		0.26–0.41	High	4	
		0.41–0.53	Moderate	3	
		0.53–0.67	Low	2	
		0.67–1.00	Very Low	1	

This study first produced the risk areas by numerically overlaying elevation, drainage density, slope, flow length, distance from the river, and NDVI. The overlay was carried out as a Boolean overlay. All criteria were combined by logical operators such as intersection (AND) and union (OR). The Ranking Method was used, where every criterion listed above was ranked according to the researcher's preference. Each factor was weighted according to the estimated significance of causing flooding. Logical operations combined the criterion maps and criterion values were generated based on a ranking method for each evaluation unit. The flood potential map was classified based on flood vulnerability: High Risk, Low Risk, Moderate Risk, Very High Risk, and Very Low Risk.

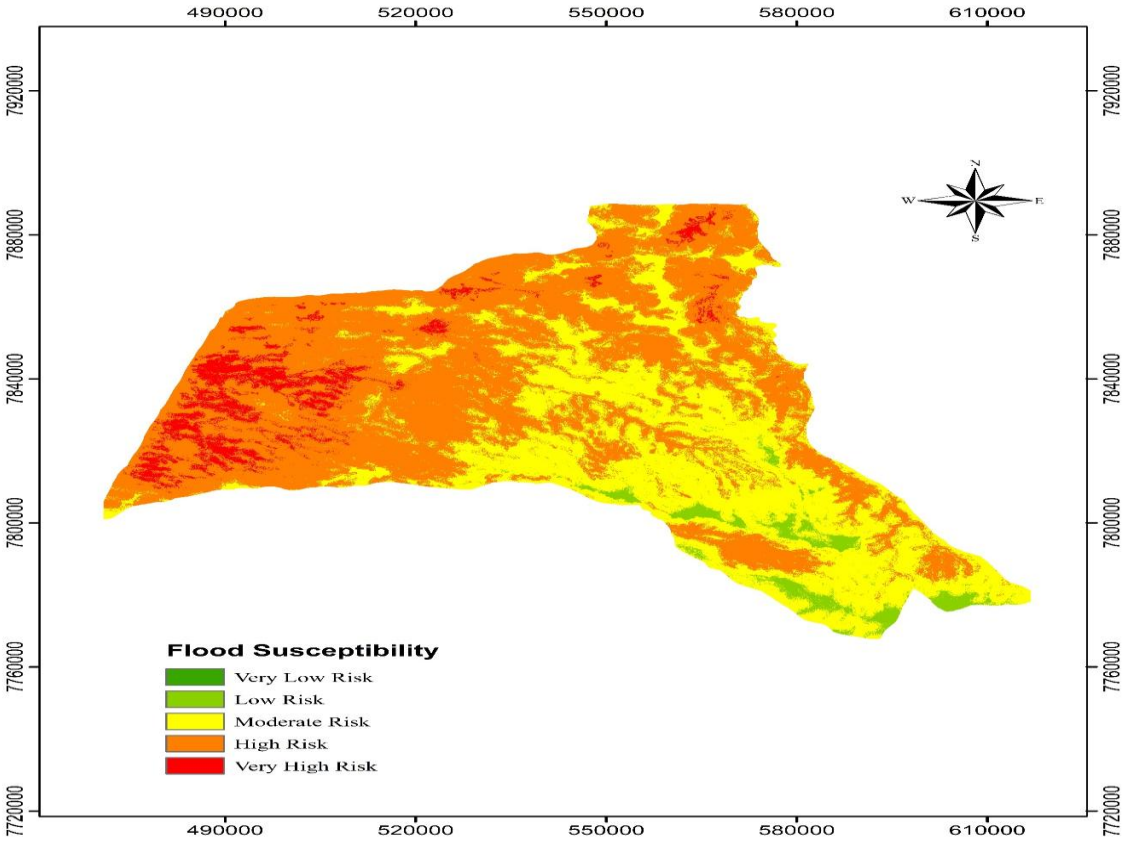

Figure 9. The Flood Susceptibility Map of Tsholotsho District

The total area of the Tsholotsho flood map was 776758.52 hectares, and 433699.57 Hectares, which is 56% of the total, were high-risk flood-prone areas. The area with a very high flood-prone risk was 41060.25 hectares (5%).

Table 5. Tsholotsho District Flood Susceptibility

Flood Susceptibility	Area (ha)	%
High Risk	433699.57	56
Low Risk	23669.74	3
Moderate Risk	278328.41	36
Very High Risk	41060.25	5
Very Low Risk	0.55	0

The results indicated that 433699.57 (56%) hectares of the Tsholotsho district are at high flood risk, and about 36% are at moderate risk.

IV. Conclusion

The flood risk assessment in Tsholotsho District reveals that natural and human factors contribute to the region's flood susceptibility. Low-lying terrain, elevation, slope, distance from the river, flow length, reduced vegetation cover, drainage density, and inadequate infrastructure amplify flood risks. These findings highlight the necessity for targeted, data-driven interventions to reduce flood risks and protect communities, infrastructure, and natural resources in Tsholotsho District.

References

[1]. Adimi, O. S. C., Tohozin, C. A. B., & Oloukoi, J. (2018). Spatial modeling and multi-criteria evaluation in determining suitable sites for maize production in Ouèssè, Benin**.** International Journal of Biological and Chemical Sciences, 12(1). https://www.journalquality.info/jpps-criteria/one-star

[2]. Ajjur, S. B., & Al-Ghamdi, S. G. (2022). Exploring urban growth–climate change–flood risk nexus in fast-growing cities. Scientific Reports, 12, Article 12265. https://doi.org/10.1038/s41598-022-16475-x

[3]. Akallouch, A., Al Mashoudi, A., Ziani, M., & Elhani, R. (2024). GIS application in urban flood risk analysis: Midar as a case study. Open Journal of Ecology, 14(2), 148–164. https://doi.org/10.4236/oje.2024.142009

[4]. Akbulut, A., Ozcevk, O., & Carton, L. J. (2018). Evaluating suitability of a GIS–AHP combined method for sustainable urban and environmental planning in Beykoz District, Istanbul. International Journal of Sustainable Development and Planning, 13(8), 1103–1115. https://doi.org/10.2495/SDP-V13-N8-1103-1115

[5]. Al-Kindi, K. M., & Alabri, Z. (2024). Investigating the role of the key conditioning factors in flood susceptibility mapping through machine learning approaches. Earth Systems and Environment, 8, 63–81. https://doi.org/10.1007/s41748-023-00369-7

[6]. Anumveh, N. N., Nkuh, R. Y., Sama, N. B., Enongene, F., Agendia, N., Kigha, P., Landoh, N., & Louis, A. (2023). Ascribing the capricious weather thesis to the unprecedented July-September 2022 flood hazards in the Kumba and Mutengene-Likomba agglomerations of the southwest Cameroon coastal plain of Cameroon. International Journal of Development Research, 13(06), 63038–63050. https://doi.org/10.37118/ijdr.26875.06.2023

[7]. Aramburú-Paucar, J. M., Martínez-Capel, F., Puig-Mengual, C. A., Muñoz-Mas, R., Bertagnoli, A., & Tonina, D. (2024). A large flood resets riverine morphology improve connectivity and enhances the habitats of a regulated river. Science of The Total Environment, 919, 170717. https://doi.org/10.1016/j.scitotenv.2024.170717

[8]. Ayenew, W. A., & Kebede, H. A. (2023). GIS and remote sensing based flood risk assessment and mapping: The case of Dikala Watershed in Kobo Woreda Amhara Region, Ethiopia. Environmental and Sustainability Indicators, 18, 100243. https://doi.org/10.1016/j.indic.2023.100243

[9]. Bhatt, G. D., Sinha, K., Deka, P. K., & Kumar, A. (2014). Flood hazard and risk assessment in Chamoli District, Uttarakhand, using satellite remote sensing and GIS techniques. International Journal of Innovative Research in Science, Engineering and Technology, 3(8), 15348–15354. https://doi.org/10.15680/IJIRSET.2014.0308039

[10]. Bora, S. L., Das, J., Bhuyan, K., & Hazarika, P. J. (2023). Flood susceptibility mapping using GIS and multi-criteria decision analysis in Dibrugarh District of Assam, North-East India. GIScience and Geo-environmental Modelling. https://doi.org/10.1007/978-3-031-15377-8. Springer Nature Switzerland AG.

[11]. Chakraborty, S., & Mukhopadhyay, S. (2019). Assessing flood risk using analytical hierarchy process (AHP) and geographical information system (GIS): Application in Coochbehar district of West Bengal, India. Natural Hazards, 99(1), 247–274. https://doi.org/10.1007/s11069-019-03737-7

[12]. Chapi, K., Singh, V. P., Shirzadi, A., Shahabi, H., Bui, D. T., Pham, B. T., & Khosravi, K. (2017). A novel hybrid artificial intelligence approach for flood susceptibility assessment. Environmental Modelling & Software, 95, 229–245. https://doi.org/10.1016/j.envsoft.2017.06.012

[13]. Dewan, A.M., Nishigaki, M and Komatsu, M (2003). Floods in Bangladesh: A Comparative Hydrological Investigation on Two Catastrophic Events. Journal of the Faculty of Environmental Science and Technology, Okayama University, Vo1.8, No.1, pp.53·62, March 2003. https://core.ac.uk/reader/12549250

[14]. Diriba, D., Takele, T., Karuppannan, S., & Husein, M. (2024). Flood hazard analysis and risk assessment using remote sensing, GIS, and AHP techniques: a case study of the Gidabo Watershed, main Ethiopian Rift, Ethiopia. Geomatics, Natural Hazards and Risk, 15(1). https://doi.org/10.1080/19475705.2024.2361813

[15]. Diriba, D., Takele, T., Karuppannan, S., & Husein, M. (2024). Flood hazard analysis and risk assessment using remote sensing, GIS, and AHP techniques: A case study of the Gidabo Watershed, main Ethiopian Rift, Ethiopia. Geomatics, Natural Hazards and Risk, 15(1). https://doi.org/10.1080/19475705.2024.2361813

[16]. Dube, E. (2017). Towards enhanced disaster risk management interventions for flood hazards and disasters in Tsholotsho District, Zimbabwe. July 2017. https://doi.org/10.13140/RG.2.2.32363.64801

[17]. Dube, E., & Mhembwe, S. (2019). Heightening gender considerations for women in flood disaster response through resource allocation and distribution in Zimbabwe. International Journal of Disaster Risk Reduction, 40, 101281. https://doi.org/10.1016/j.ijdrr.2019.101281

[18]. Dube, E., Mtapuri, O., & Matunhu, J. (2018). Flooding and poverty: Two interrelated social problems impacting rural development in Tsholotsho District of Matabeleland North Province in Zimbabwe. Jàmbá: Journal of Disaster Risk Studies, 10(1), a455. https://doi.org/10.4102/jamba.v10i1.455

[19]. Dube, E., Mtapuri, O., & Matunhu, J. (2018). Flooding and poverty: Two interrelated social problems impacting rural development in Tsholotsho district of Matabeleland North province in Zimbabwe. Jamba: Journal of Disaster Risk Studies, 10(1). https://doi.org/10.4102/jamba.v10i1.455

[20]. Dube, E., Mtapuri, O., & Matunhu, J. (2018). Managing flood disasters on the built environment in the rural communities of Zimbabwe: Lessons learned. Jàmbá: Journal of Disaster Risk Studies, 10(1), a542. https://doi.org/10.4102/jamba.v10i1.542

[21]. Dube, E., Wedawatta, G., & Ginige, K. (2021). Building-back-better in post-disaster recovery: Lessons learned from Cyclone Idai-induced floods in Zimbabwe. International Journal of Disaster Risk Science, 12, 700–712. https://doi.org/10.1007/s13753-021-00373-3

[22]. El-Fakharany, M. A., & Mansour, N. M. (2021). Morphometric analysis and flash floods hazards assessment for Wadi Al Aawag drainage basins, southwest Sinai, Egypt. Environmental Earth Sciences, 80, 168. https://doi.org/10.1007/s12665-021-09457-1

[23]. Floodlist (2017). Zimbabwe – Hundreds were displaced as the flood threat continued. European Centre for Medium-Range Weather Forecasts. Retrieved from https://floodlist.com/africa/zimbabwe-floods-february-march-2017

[24]. Gaston, B. W. (2009). Geographic information systems-based demarcation of risk zones: The case of the Limbe Sub-Division – Cameroon. Journal of Disaster Risk Studies, 2(1), 54–79. https://hdl.handle.net/10520/EJC51155

[25]. Goepel, K.D. (2013) Implementing the Analytic Hierarchy Process as a Standard Method for Multi-Criteria Decision Making In Corporate Enterprises—A New AHP Excel Template with Multiple Inputs. Proceedings of International Symposium on the Analytic Hierarchy Process, Kuala Lumpur, 23-36 June 2013, 1-10. https://bpmsg.com/

[26]. Government of India (2008). National Disaster Management Guidelines. Management of Floods. National Disaster Management Authority. Government of India. https://nidm.gov.in/PDF/guidelines/floods.pdf

[27]. Government of India (2023). Flood Affected Area Atlas of India (1998-2022) - Satellite-based study. Version -1 (1998-2022). https://www.nrsc.gov.in/sites/default/files/pdf/DMSP/FloodAffectedAreaAtlas_Digital.pdf

[28]. Government of Zimbabwe (GOZ) (2017). Zimbabwe: Inter-Agency Flooding Rapid Assessment Report Tsholotsho District, 23 - 24 February 2017. https://reliefweb.int/report/zimbabwe/zimbabwe-inter-agency-flooding-rapid-assessment-report-tsholotsho-district-23-24

[29]. Government of Zimbabwe (2019). Zimbabwe Rapid Impact and Needs Assessment (RINA). https://documents1.worldbank.org/curated/fr/714891568893029852/pdf/Zimbabwe-Rapid-Impact-and-Needs-Assessment-RINA.pdf

[30]. Gu, X., & Liu, X. (2024). Planning scale flood risk assessment and prediction in ultra-high density urban environments: The case of Hong Kong. Ecological Indicators, 162, Article 112000. https://doi.org/10.1016/j.ecolind.2024.112000

[31]. Gwimbi, P. (2007). The effectiveness of early warning systems for reducing flood disasters: Some experiences from cyclone-induced floods in Zimbabwe. Journal of Sustainable Development in Africa, 9(4), 1520–5509. https://www.jsd-africa.com/Jsda/V9n4_Winter2007/PDF/EfectivenessEalierWarningSystem.pdf

[32]. Hagos, Y. G., Andualem, T. G., Yibeltal, M., & Mengie, M. A. (2022). Flood Hazard Assessment and Mapping Using GIS Integrated with Multi-Criteria Decision Analysis in Upper Awash River Basin, Ethiopia. Applied Water Science, 12, 1-18. https://doi.org/10.1007/s13201-022-01674-8

[33]. Karna, B. K., Shrestha, S., & Koirala, H. L. (2023). GIS-based approach for suitability analysis of residential land use. Geographical Journal of Nepal, 16(1). https://doi.org/10.3126/gjn.v16i01.53483

[34]. Kaya, C. M., & Derin, L. (2023). Parameters and methods used in flood susceptibility mapping: A review. Journal of Water and Climate Change, 14(6), 1935–1960. https://doi.org/10.2166/wcc.2023.035

[35]. Kourgialas, N. N., & Karatzas, G. P. (2011). Flood management and a GIS modeling method to assess flood-hazard areas—a case study. Hydrological Sciences Journal, 56(2), 212–225. https://doi.org/10.1080/02626667.2011.555836

[36]. Li, C. J., Chai, Y. Q., Yang, L. S., & Li, H. R. (2016). Spatio-temporal distribution of flood disasters and analysis of influencing factors in Africa. Natural Hazards, 82, 721–731. https://doi.org/10.1007/s11069-016-2181-8

[37]. Liuzzo, L., Sammartano, V., & Freni, G. (2019). Comparison between different distributed methods for flood susceptibility mapping. Water Resources Management, 33, 3155–3173. https://doi.org/10.1007/s11269-019-02293-w

[38]. Ma, S., Wang, L.-J., Jiang, J., & Zhao, Y.-G. (2024). Land use/land cover change and soil property variation increased flood risk in the black soil region, China in the last 40 years. Environmental Impact Assessment Review, 104, 107314. https://doi.org/10.1016/j.eiar.2023.107314

[39]. Manyangadze, T., Mavhura, E., Mudavanhu, C., & Pedzisa, E. (2022). Flood inundation mapping in data-scarce areas: A case of Mbire District, Zimbabwe. Geo: Geography and Environment, 9, e00105. https://doi.org/10.1002/geo2.105

[40]. Mitra, R., & Das, J. (2023). A comparative assessment of flood susceptibility modeling of GIS-based TOPSIS, VIKOR, and EDAS techniques in the Sub-Himalayan foothills region of Eastern India. Environmental science and pollution research international, 30(6), 16036–16067. https://doi.org/10.1007/s11356-022-23168-5

[41]. Mojaddadi, H., Pradhan, B., Nampak, H., Ahmad, N., & Ghazali, A. H. B. (2017). Ensemble machine-learning-based geospatial approach for flood risk assessment using multi-sensor remote-sensing data and GIS. Geomatics, Natural Hazards and Risk, 8(2), 1080–1102. https://doi.org/10.1080/19475705.2017.1294113

[42]. Molnar-Tanaka, K. and Surminski, S (2024). "Nature-based solutions for flood management in Asia and the Pacific," OECD Development Centre Working Papers, No. 351, OECD Publishing, Paris, https://doi.org/10.1787/f4c7bcbe-en.

[43]. Natkaniec, W., & Godyń, I. (2024). Urban flood risk assessment and mapping using GIS-DEMATEL method: Case of the Serafa River watershed, Poland. Water, 16(18), 2636. https://doi.org/10.3390/w16182636

[44]. Ngulube, N. K., Tatano, H., & Samaddar, S. (2024). Factors impacting participatory post-disaster relocation and housing reconstruction: The case of Tsholotsho District, Zimbabwe. International Journal of Disaster Risk Science, 15, 58–72. https://doi.org/10.1007/s13753-024-00536-y

[45]. Nji, T. M., Balgah, R. A., & Vubo, E. Y. (2019). Coping with flood hazards in Cameroon: The role of community-based strategies. Sociology International Journal, 3(5). https://medcraveonline.com/SIJ/coping-with-flood-hazards-in-cameroon-the-role-of-community-based-strategies.html

[46]. Nyoni, C., Muzembi, B. B., Mhlanga, M., Mureriwa, D., Jaji, F., & Muzire, M. (2019). Tsholotsho flood survivors: Three years on after the disaster caused by Cyclone Dineo. The Fountain – Journal of Interdisciplinary Studies, 3(1), 57. https://journals.cuz.ac.zw/index.php/fountain/article/view/151/68

[47]. OECD, (2024). Nature-based solutions for flood management in Asia and the Pacific. Working paper. https://www.oecd.org/en/publications/nature-based-solutions-for-flood-management-in-asia-and-the-pacific_f4c7bcbe-en.html

[48]. Osman, S., & Das, J. (2023). GIS-based flood risk assessment using multi-criteria decision analysis of Shebelle River Basin in southern Somalia. SN Applied Sciences, 5(5), 1–17. https://doi.org/10.1007/s42452-023-05360-5

[49]. Rahman, M. M., Shobuj, I. A., Islam, Md. R., Islam, Md. R., Hossain, Md. T., Alam, E., … Islam, M. K. (2024). Flood preparedness in rural flood-prone area: a holistic assessment approach in Bangladesh. Geomatics, Natural Hazards and Risk, 15(1). https://doi.org/10.1080/19475705.2024.2379599

[50]. Rahman, Z. U., Ullah, W., Bai, S., Ullah, S., Jan, M. A., Khan, M., & Tayyab, M. (2023). GIS-based flood susceptibility mapping using bivariate statistical model in Swat River Basin, Eastern Hindukush region, Pakistan. Frontiers in Environmental Science, 11. https://doi.org/10.3389/fenvs.2023.1178540

[51]. Saaty, T. L. (1997). A scaling method for priorities in hierarchical structures. Journal of Mathematical Psychology, 15(3), 234–281. http://dx.doi.org/10.1016/0022-2496(77)90033-5

[52]. Saaty, T. L. (2008). Decision making with the analytic hierarchy process. International Journal of Services Sciences, 1(1), 83–98. https://doi.org/10.1504/IJSSCI.2008.017590

[53]. Saha, S., Gayen, A., & Bayen, B. (2022). Deep learning algorithms to develop flood susceptibility map in data-scarce and ungauged river basin in India. Stochastic Environmental Research and Risk Assessment, 36, 3295–3310. https://doi.org/10.1007/s00477-022-02195-1

[54]. Samu, R., & Kentel, A. S. (2018). An analysis of Zimbabwe's flood management and mitigation measures for a sustainable future. International Journal of Disaster Risk Reduction, 31, 691–697. https://doi.org/10.1016/j.ijdrr.2018.07.013

[55]. Shahabi, A., Nabiollahi, K., Davari, M., Zeraatpisheh, M., Heung, B., Scholten, T., & Taghizadeh-Mehrjardi, R. (2022). Spatial prediction of soil properties through hybridized random forest model and combination of reflectance spectroscopy and environmental covariates. Geocarto International, 37(27), 18172–18195. https://doi.org/10.1080/10106049.2022.2138565

[56]. Siam, Z. S., Hasan, R. T., Anik, S. S., Noor, F., Adnan, M. S. G., Rahman, R. M., & Dewan, A. (2022). National-scale flood risk assessment using GIS and remote sensing-based hybridized deep neural network and fuzzy analytic hierarchy process models: a case of Bangladesh. Geocarto International, 37(26), 12119–12148. https://doi.org/10.1080/10106049.2022.2063411

[57]. Sibanda, N., & Matsa, M. M. (2020). Flood disaster preparedness and response in Zimbabwe: A case study of Tsholotsho District, Zimbabwe. International Journal of Disaster Response and Emergency Management, 3(2), 35–47. https://doi.org/10.4018/IJDREM.2020070103

[58]. Siefi, S., Karimi, H., Soffianian, A. R., & Pourmanafi, S. (2017). GIS-based multi-criteria evaluation for thermal power plant site selection in Kahnuj County, SE Iran. Civil Engineering Infrastructures Journal, 50(1), 179–189. https://doi.org/10.7508/ceij.2017.01.011

[59]. Singh, O & Kumar, M (2017). Flood occurrences, damages, and management challenges in India: a geographical perspective. Arabian Journal of Geosciences. Volume 10, Number 5. DOI 10.1007/s12517-017-2895-2.

[60]. Subraelu, P., Ahmed, A., Ebraheem, A. A., Sherif, M., Mirza, S. B., Ridouane, F. L., & Sefelnasr, A. (2023). Risk Assessment and Mapping of Flash Flood Vulnerable Zones in Arid Region, Fujairah City, UAE-Using Remote Sensing and GIS-Based Analysis. Water, 15(15), 2802. https://doi.org/10.3390/w15152802

[61]. Tehrany, M. S., Pradhan, B., & Jebuv, M. N. (2013). A comparative assessment between object and pixel-based classification approaches for land use/land cover mapping using SPOT 5 imagery. Geocarto International, 29(4), 351–369. https://doi.org/10.1080/10106049.2013.768300

[62]. Tirivangasi, M. H., Nyahunda, L., & Mabila, T. E. (2021). Review of disaster response strategies for sustainable development in the wake of flood risks in Zimbabwe's rural-urban settlements. Technium Social Sciences Journal, 26, 968–983. https://techniumscience.com/index.php/socialsciences/index

[63]. Tshuma, M. (2021). Community characteristics influencing flood recovery: A case of Sipepa and Jimila wards in Tsholotsho District, Zimbabwe, during the 2016 to 2017 floods. International Research Journal of Arts and Social Science, 9(4), 1–11. Available at: http://www.interesjournals.org/IRJASS

[64]. Tshuma, M., Belle, J. A., & Ncube, A. (2023). An analysis of factors influencing household water, sanitation, and hygiene (WASH) experiences during flood hazards in Tsholotsho District using a seemingly unrelated regression (SUR) model. Water, 15(371). https://doi.org/10.3390/w15020371

[65]. Twumasi, Y., Merem, E., Namwamba, J., Okwemba, R., Ayala-Silva, T., Abdollahi, K., Lukongo, O., Tate, J., Cour-Conant, K., & Akinrinwoye, C. (2020). Use of GIS and remote sensing technology as a decision support tool in flood disaster management: The case of Southeast Louisiana, USA. Journal of Geographic Information System, 12(2), 141–157. https://doi.org/10.4236/jgis.2020.122009

[66]. UNICEF (2024). Bangladesh Situation Report No. 1 (Flash Floods in Northern and Southeastern regions), 27 August 2024. https://www.unicef.org/documents/bangladesh-situation-report-no-1-flash-floods-northern-and-southeastern-regions-27-august

[67]. UNICEF (2024). Cameroon Floods. Flash Update 02. https://www.unicef.org/media/162071/file/Cameroon-Floods-Flash-Update-18-September-2024.pdf

[68]. Vijith, H., & Satheesh, R. (2006). GIS-based morphometric analysis of two major upland sub-watersheds of Meenachil River in Kerala. Journal of the Indian Society of Remote Sensing, pp. 34, 181–185. https://doi.org/10.1007/BF02991823

[69]. Wantim, M. N., Peter, N. F., Eyong, N. J., Zisuh, A. F., Yannah, M., Lyonga, M. R., Yenshu, E. V., & Ayonghe, S. N. (2022). Flood hazard and its associated health impacts in Limbe Health District, Cameroon. African Journal of Health Sciences, 35(4), July-August 2022.

[70]. Wantim, M. N., Zisuh, A. F., Tendong, N. S., Mbua, R. L., Findi, E. N., & Ayonghe, S. N. (2023). Strategies and perceptions towards flood control and waste management in Limbe city, Cameroon. Jàmbá: Journal of Disaster Risk Studies, 15(1), a1390. https://doi.org/10.4102/jamba.v15i1.1390

[71]. Wondim, Y. K. (2016). Flood hazard and risk assessment using GIS and remote sensing in Lower Awash Sub-basin, Ethiopia. Journal of Environment and Earth Science, 6(9). https://core.ac.uk/download/pdf/234664703.pdf

[72]. World Bank (2019). Mozambique. Disaster Risk Profile. https://documents1.worldbank.org/curated/en/845611574234249644/pdf/Disaster-Risk-Profile-Mozambique.pdf

[73]. Wu, J., & Liang, L. (2012). A multiple criteria ranking method based on game cross-evaluation approach. Annals of Operations Research, 197(1), 191–200. https://doi.org/10.1007/s10479-010-0817-8

[74]. Wudineh, F. A. (2023). Land-use and land-cover change and its impact on flood hazard occurrence in Wabi Shebele River Basin of Ethiopia. Hydrology Research, 54(6), 756–769. https://doi.org/10.2166/nh.2023.121

[75]. Zimbabwe Human Rights Commission (2015). Report on the Mission Visit to Tsholotsho to Assess the Human Rights Situation of Flood-Affected Communities. https://ntjwg.uwazi.io/en/entity/sughg7dtph?page=1

[76]. Zimstat (2022). Zimbabwe 2022 Population and Housing Census. https://www.zimstat.co.zw/wp-content/uploads/Demography/Census/2022_Population_Distribution_by_District_Ward_SexandHouseholds_23012023.pdf

[77]. Ziwei, L., Xiangling, T., Liju, L., Yanqi, C., Xingming, W., & Dishan, Y. (2023). GIS-based risk assessment of flood disaster in the Lijiang River Basin. Scientific Reports, pp. 13, 6160. https://doi.org/10.1038/s41598-023-32829-5